# Growth of Polyelectrolyte Complex Nanoparticles: Computer Simulations and Experiments

**ARTICLE** *in* THE JOURNAL OF PHYSICAL CHEMISTRY C · JUNE 2008

Impact Factor: 4.77 · DOI: 10.1021/jp800581y



**3 AUTHORS:**

Vitaliy Starchenko
University of Florida
**16** PUBLICATIONS **56** CITATIONS
SEE PROFILE

Martin Müller
Leibniz Institute of Polymer Research Dres…
**127** PUBLICATIONS **1,791** CITATIONS
SEE PROFILE

Nikolai I Lebovka
Biocolloidal Chemistry Institute named aft…
**363** PUBLICATIONS **3,174** CITATIONS
SEE PROFILE

# Growth of Polyelectrolyte Complex Nanoparticles: Computer Simulations and Experiments

**Vitaliy Starchenko,[†,‡] Martin Müller,[*,†] and Nikolai Lebovka[‡]**

*Leibniz Institute of Polymer Research Dresden e.V., Hohe Strasse 6, 01069 Dresden, Germany, and Institute of Biocolloidal Chemistry named after F. D. Ovcharenko, NAS of Ukraine, 42, Boulevard Vernadskogo, Kyiv 03142, Ukraine*

*Received: January 21, 2008; Revised Manuscript Received: March 7, 2008*

Herein we report on simulation and experimental studies on the formation of monomodal polyelectrolyte complex (PEC) nanoparticles, prepared by mixing two solutions of oppositely charged polyelectrolytes (PELs) under variation of ionic strength and applying centrifugation. This work aims at the better understanding of recently reported experimental studies, which demonstrated that consecutive centrifugation results in the removal of small primary PEC particles in polymodal dispersions and receipt of monomodal PEC dispersions of secondary PEC particles. In order to describe this effect and the possibilities of particle size regulation in PEC dispersions, a novel particle coagulation model, based on the combination of the mean-field theory of Smoluchowski and the Fuchs stability approach including a classical DLVO potential of interparticle interactions, was used in this study. The aggregation process was simulated under variation of the typical colloidal parameters: the Hamaker constant $A$, the Debye length $\lambda$, and the $\zeta$-potential. The influence of these parameters on the mean final size, kinetics, and size distribution function of the colloid particles was studied. In the experimental section we study the system of cationic poly(diallyldimethylammonium chloride) (PDADMAC) mixed with an excess of anionic sodium poly(styrenesulfonate) (PSS) and varying NaCl concentration in the range $C_{NaCl} = 0.001–0.05$ M. The size of secondary PEC particles as a function of the salt concentration exhibited a pronounced minimum at $C_{NaCl} \approx 0.005$ M. The influence of PEL conformation on the PEC particle size and the comparability of simulation and experimental results are discussed.

## Introduction

Polymer nanoparticles, such as polymer conjugates,[1] liposomes,[2] and hollow capsules,[3] find increasing interest as carriers for drugs, proteins, and DNA in pharmaceutical, biomedical, and food applications. Key factors for preparation and application of the appropriate nanoparticles are reproducible preparation protocol, monomodality, and the possibility to obtain particles of determined and graded sizes. Polyelectrolyte complexes (PECs) might be promising for these purposes, but poor reproducibility of the formation process and polydisperse size distributions were frequently observed in the past. However, recently an improved concept of PEC allowing elimination of the said disadvantages was proposed.[4,5] The raw PEC dispersions, obtained by mixing cationic poly(diallyldimethylammonium chloride) (PDADMAC) and anionic poly(maleic acid-*co*-α-methylstyrene) (PMA−MS) solutions in nonstoichometric ratios ($n_-/n_+ = 1.50$ or 0.66 with respect to charged units) were treated by consecutive centrifugation/separation steps. It allowed significant decrease of the polydispersity of the system and elimination of the fraction of small primary complexes with particle radii of about 10 nm. As a result, the secondary particles with radii of about 100 nm prevailed in dispersion. This was shown by dynamic light scattering (DLS) and atomic force microscopy (AFM) and was further analyzed by colloid titration and Fourier transform infrared (FTIR) spectroscopy. However, the following questions remain open: Do PEC particles stop growing at reaching a certain size and is this size unique for a given system? Is it possible to apply the DLVO approach to simulate the PEC formation process? How does the particle size depend on the salt content? In this paper we address these questions, aiming at a deeper understanding of the PEC formation process.

This study is based on the assumption that PEC dispersions consist of secondary particles, which were formed through aggregation of the primary particles. This formation process, the final structure, size, and distribution functions of the PEC particles, are supposed to be controlled by the competition of long-range electrostatic and short-range dispersive interactions.

Different theoretical methods can be used for the description of aggregation in such systems. It is difficult to apply the classical mean-field rate equations of Smoluchowski, because distribution of the particle radii and charges results in complex rate kernels and restricts the possibility of analytical solutions. Moreover, the mean-field approach was shown to be appropriate for prediction of different average cluster quantities, but it failed to describe fluctuations and size distributions in aggregating systems.[6] Our understanding of the aggregation processes occurring in a complex system with distribution of sizes, charges, and other material properties of particles can be substantially improved by using different computer techniques, such as Brownian dynamics, the Monte Carlo model, and the population balance model[6–14] for simulation of the aggregation kinetics. The aggregation of charged particles can be approximated by the slow coagulation model, but this approach requires further refinement, accounting for distribution of the Fuchs stability ratio,[15] which is present in real systems.

Our paper is structured as follows. First, the simulation section describes the general Monte Carlo approach for investigation of the aggregation of charged particles with distributed stability

* Corresponding author. Phone: +49-351-4658-405. Fax:+49-351-4658-284. E-mail: mamuller@ipfdd.de.
† Leibniz Institute of Polymer Research Dresden.
‡ NAS of Ukraine.

10.1021/jp800581y CCC: $40.75 
Published on Web 05/24/2008

ratios. The approach is based on the combination of classical Smoluchowski and Fuchs stability theories. Second, the experimental section contains a description of the preparation and characterization of the PEC particles of the poly(diallyldimethylammonium chloride) (PDADMAC)/poly(styrenesulfonate) (PSS) system under variation of the NaCl concentration. Finally, we demonstrate the ability of the simulation technique to provide a reasonable description of the aggregation processes consistent with the obtained experimental data.

## Materials and Methods

**Computer Simulation.** The model used for simulation is similar to that proposed in ref 8, which was shown to be applicable for simulation of Smoluchowski's aggregation processes. Initially, all particles were of the same sort (primary) and were randomly located in the sites of a three-dimensional cubic lattice of size $L \times L \times L$. Most of the simulations were carried out using the systems with $L = 50$. In order to reduce statistical errors, the results of different runs (typically 100) were averaged. The accepted size and number of runs allowed reaching a reasonable precision of the data calculation. The periodical boundary conditions were applied. The initial number of particles in the system was $N_o = p_o L^3$, where $p_o$ is the initial filling fraction of the sites. Diffusion motion of the particles was modeled by random walks; i.e., it was assumed that a randomly selected particle can move in one of the six possible directions at a distance between near-neighbor lattice sites.

In a case of fast aggregation, the particles were aggregated at the first contact. When a particle was getting into a site filled with another particle, these two particles aggregated and a new larger particle arose in the site. Such an approach implying coalescence of two particles into a single one is similar to that proposed in ref 9. The aggregation was assumed to be irreversible without any breakdown of clusters. The two primary particles were forming a dimer, a primary particle and a dimer were forming a trimer, etc., and the total number of particles $N$ decreased with time $t$.

Approximations of the computer simulation model used in our work assumed the compact structure of clusters. This approximation seems to be reasonable as far as the previous study showed that shape of PEC particles was nearly spherical without visible presence of any ramification.[4,5] Therefore, the effects of ramification and possible cluster fractality were neglected at this stage. It was assumed that an aggregate had a spherical form, and its radius $r$ was calculated as

$$r = r_p n^{1/3} \tag{1}$$

where $r_p$ is the radius of a primary particle and $n$ is a number of the primary particles in an aggregate.

The probability of the particle movement $f$ was taken to be proportional to the translational diffusion coefficient of the particle $D$. The Stokes–Einstein relationship states that $D$ is inversely proportional to the particle radius $r$ as

$$D = kT/6\pi r\eta \tag{2}$$

where $k = 1.381 \times 10^{-23}$ J/K, $T$, and $\eta$ stand for the Boltzmann constant, absolute temperature, and solvent viscosity, respectively. Hence, the probability of the particle movement depended on the number of primary particles in an aggregate as

$$f \propto D \propto r^{-1} n^{-1/3} \tag{3}$$

The time step d$t$ in the Monte Carlo procedure was calculated similarly as described in ref 8. After each attempted move with the probability of $f = (n_{min}/n)^{1/3}$, the time was increased by d$t$ $= n_{min}^{1/3}/N(t)$, where $n_{min}^{1/3}$ was the number of primary particles in an aggregate of a minimal size, and $N(t)$ was the number of particles present at time $t$. For the case of slow, or restricted, aggregation, the probability $w$ of two-particle aggregation (sticking probability) was calculated from the Fuchs theory as[15,16]

$$w = \left((r_1 + r_2) \int_{r_1+r_2}^{\infty} \exp[u(s)/kT]/G(s)s^2\, ds\right)^{-1} \tag{4}$$

where $r_1$ and $r_2$ are the radii of the particles, $s$ is the distance between centers of the particles, and $G(s)$ is the hydrodynamic correction factor for two spheres approaching each other, which represents the relative mutual diffusion coefficient. The simple relations for this factor can be found in the literature.[15] For particles smaller than 100 nm in diameter, the electroviscous coupling is also essential, and the correction factor should be modified.[17] Exact relations for $G(s)$ for the asymmetric situation with unequal spheres are still unknown, and in this work we neglect hydrodynamic and electroviscous corrections and put $G(s) = 1$.

According to the DLVO theory,[18] the total energy of interaction $u$ between two spherical particles of different sizes was approximated by the sum of contributions of the van der Waals attraction $u_a$ and electrostatic repulsion $u_r$:[19]

$$u_a = -\frac{A}{6}\left(\frac{2r_1r_2}{s^2-(r_1+r_2)^2} + \frac{2r_1r_2}{s^2-(r_1-r_2)^2} + \ln\left[\frac{s^2-(r_1+r_2)^2}{s^2-(r_1-r_2)^2}\right]\right) \tag{5a}$$

$$u_r = 4\pi\varepsilon\varepsilon_0\xi^2 \ln(1+\exp((r_1+r_2-s)/\lambda))r_1r_2/(r_1+r_2) \tag{5b}$$

where $A$ is the Hamaker constant, $\varepsilon$ and $\varepsilon_0$ are the dielectric constants of the medium and vacuum, respectively, $\zeta$ is the zeta-potential, and $\lambda$ is the Debye length. Approximation for electrostatic repulsion in eq 5b is valid for relatively small values of $\zeta$, $\zeta/z < 50$ mV, where $z$ is the valence of electrolyte ions. Hence, the initial sticking probability $w_p$ was the same for all the particles and depended on the primary particle size $r_p$ and different parameters of the interparticle potential ($A$, $\zeta$-potential, $\lambda$). The larger particles were formed during aggregation, and the sticking probability calculated from eq 4 was a function of the radii of sticking species, $r_1$ and $r_2$. The constant rate mean-field Smoluchowski approach predicts the following time evolutions of the total number of particles:[20]

$$N/N_o = (1 + t/\theta)^{-1} \tag{6}$$

Here, $\theta$ is the half-coagulation time corresponding to $N = N_o/2$. The computation model implying that the sticking probability $w$ is constant and equals unity (the model of fast aggregation) was tested for consistency with the Smoluchowski theory. Figure 1 shows examples of the calculated dependences of the relative number of particles $N/N_o$ versus reduced time $t/p_o$ at different values of the initial filling fraction $p_o$. The computed data were satisfactorily fitted by eq 6 at $N/N_o > 0.1$ and $p_o$ between $10^{-4}$ and $10^{-1}$. The estimated value of "computer" half-coagulation time was

$$\theta = (1.56 \pm 0.01)/p_o \tag{7}$$

which holds for models with constant and variable rates.

The computer experiment overestimates values of $N/N_o$ as compared with analytical predictions of eq 6 at a long time $t$,

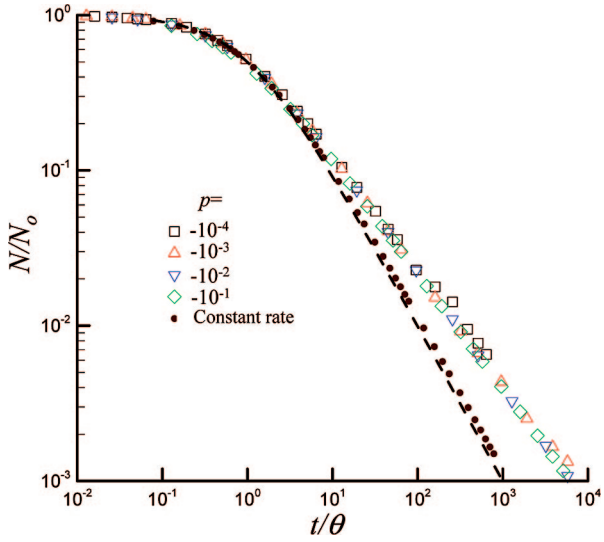


**Figure 1.** Relative number of particles $N/N_o$ versus reduced time of aggregation $t/\theta$ at different values of initial filling fractions $p_o$. The filled circles were obtained from simulation in the constant rate approximation at $p_o = 0.1$, and the dashed line corresponds to eq 6.

$t \geq 10$. Note that the simplest form of the constant rate Smoluchowski theory was based on the assumption that the rate of aggregation was constant and independent of the size of the aggregated particles. In fact, this approximation is not valid for long times $t$ ($>\theta$), when the size distribution of particle is essential (see, e.g., ref 8). Simulation of the "artificial" constant rate process with elimination of any size dependence of the aggregation process was done in order to check consistency with the analytical prediction of eq 6. A similar simulation was analyzed earlier for a nonlattice problem.[8] The filled circles (Figure 1), simulated by the constant rate model, do not deviate noticeably from the theoretical dashed line, obtained from eq 6. It confirms the adopted scheme of simulation.

For a colloidal dispersion, the "real" half-coagulation time $\theta$ may be estimated as[20]

$$\theta = r_p^2/6D\phi = \tau/\phi \quad (8)$$

Here, $\varphi$ is the volume fraction of the primary particles, and $\tau = r_p^2/6D$ is the Brownian time. During the Brownian time, the length of diffusion of a primary particle is equal to its radius $r_p$. Assuming that $\eta \sim 0.001$ Pa·s (the water viscosity at temperature $T = 298$ K is equal to $\eta = 0.000\,891$ Pa·s[21]) and $r_p = 10$ nm, the following estimation can be obtained at the room temperature: $\tau = r_p^{2/6}D = \pi r_p^3\eta/kT \approx 0.76 \times 10^{-6}$ s. In all the calculations, the temperature $T$ was kept constant at $T = 298$ K, the initial filling fraction $p_o$ was 0.1, and the radius of primary particles was fixed at $r_p = 10$ nm.[4]

**Experimental Section.** ***Polyelectrolyte Solutions.*** The polycation (PC) poly(diallyldimethylammonium chloride) (PDADMAC) (20% water solution Aldrich Chemical Co., Inc., Milwaukee, WI) (Figure 2a) and the polyanion (PA) poly(styrenesulfonic acid) (PSS) (Polysciences, Inc., Warrington, PA) (Figure 2b) were used for formation of the PEC dispersions.

PDADMAC with molecular weight within $M_w^{PDADMAC} = 200\,000$–$350\,000$ g/mol and PSS with molecular weight $M_w^{PSS} = 4\,600$ g/mol were used in all experiments. The PEL solutions were prepared using deionized refined water (Millipore GmbH, Eschborn, Germany) with equal PEL concentration of $C_{PEL} = 0.001$ M. The salt concentration $C_s$, or ionic strength $I$, of the PEL solutions was adjusted by variation of the NaCl (Merck KG, Darmstadt, Germany) concentration $C_s = 0.001$, 0.002, 0.005, 0.01, 0.02, 0.05, and 0.075 M.

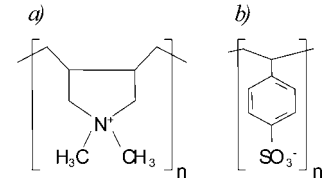


**Figure 2.** Structural formulas of polyelectrolytes: (a) poly(diallyldimethylammonium chloride); (b) poly(styrenesulfonate).

***Preparation of PDADMAC/PSS Nanoparticles.*** PEL solutions of equal PEL concentration ($C_{PA} = C_{PC}$) and salt concentration ($C_{PC}^{NaCl} = C_{PA}^{NaCl}$) were mixed in a glass beaker using a home-built device consisting of a peristaltic pump and a stirring panel. The salt was added to PEL solution before mixing. The stoichiometric mixing ratio, related to the charged monomer units, was $n_-/n_+ = 1.5$. Typically, 10 mL of PDADMAC solution (minority component) was added dropwise to 15 mL of PSS solution (excess component) under continuous stirring during 20 min.

***Dynamic Light Scattering.*** The sizes of PEC particles were checked by dynamic light scattering (DLS). DLS data were recorded by a Zetasizer 3000 (632.8 nm, 10 mW He−Ne Laser, Malvern Instruments, Worcestershire, U.K.) and a Nano S 633 (Malvern Instruments Ltd.) applying the scattering angle of 90°. The samples were held in 10 mm cuvettes. The mean particle radius $r_m$ was estimated as the hydrodynamic radius using the Stokes–Einstein equation. The shown errors are related to the standard deviation of, at least, three different measurements.

## Results and Discussion

**Simulation Results.** The Fuchs extension of the Smoluchowski theory to slow aggregation predicts the same functional form of $r_m(t)$ dependence with increased value of the half-coagulation time, when it is multiplied by the factor $1/w$. It is assumed that $w$ is equal to the initial aggregation probability $w_p$, calculated from eq 4at $r_1 = r_2 = r_p$, where $r_p$ is the primary particle radius. Figure 3 presents the mean radius of a particle $r_m$ versus scaled time $w_p t/\theta$, which were numerically estimated for different initial values of the aggregation probability $w_p$ (which corresponds to the different combinations of the Debye length $\lambda$ and Hamaker constant $A$). Note that the simulation data for the constant diffusion coefficients (open squares in Figure 3) fairly correspond to the constant rate Smoluchowski theory at fast aggregation with $w = w_p = 1$, which predicts $r_m = r_p(1 + t/\theta)^{1/3}$ (dashed line in Figure 3).

The values of $r_m$ were a continuously increasing function of time within the limit of $t/\theta \leq 10^{11}$ available in our simulation. However, the dependences of $r_m(t/\theta)$ for the slow (electrostatically restricted) growth model exhibited a certain tendency to saturation at long times of aggregation ($t/\theta$) $\gg$ 1). Such saturation behavior reflects the limitation of the growth of large-sized particles, which is controlled by electrostatic repulsion interactions. The inhibition of the large-sized aggregate formation was previously observed for the Eden model for particles interacting via long-range Coulomb repulsion and short-range attraction.[22,23] The simulation predicts that strengthening of electrostatic repulsion can result in a decreased compactness of the clusters and development of branched morphologies.[22,23] A similar conclusion about chainlike fractal internal structure of particles, formed by electrostatic heteroaggregation, was made from

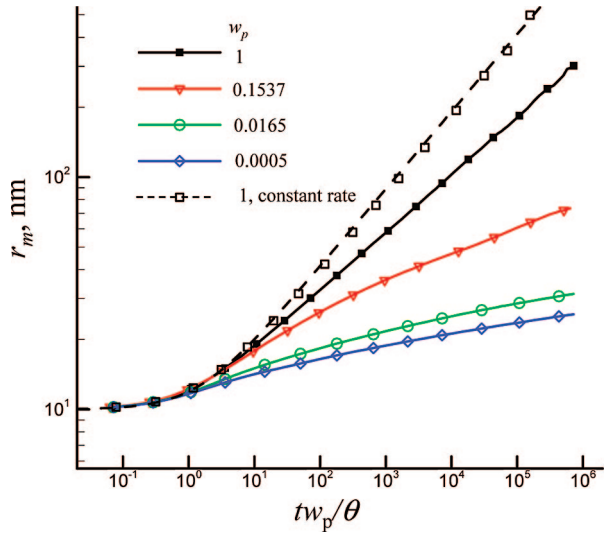


**Figure 3.** Mean particle radius $r_m$ versus scaled time $w_p t/\theta$, estimated at $A = 1 \times 10^{-20}$ J and $\zeta = -40$ mV, for different initial values of the aggregation probability $w = w_p = 1 =$ constant (model of fast aggregation), $w_p = 0.1537$ ($\lambda = 1$ nm), $w_p = 0.0165$ ($\lambda = 2$ nm), and $w_p = 0.0005$ ($\lambda = 9$ nm). Dashed line corresponds to the model of fast aggregation ($w = w_p = 1$) with constant rate; i.e., diffusion coefficient was set constant irrespectively of the size of particle.

Brownian dynamics simulation and experimental investigation.[24] Noncompact structure of an aggregate can affect the time dependence of the mean particle radius $r_m$, but present calculations were limited by consideration of compact structures.

Additionally, Figure 3 demonstrates that the constant rate approximation for the fast aggregation (open squares) results in an overestimation of the mean radius of a particle compared with the same case for the size-dependent diffusion coefficient (filled squares). Moreover, the simulated data show a noticeable deviation of $r_m(w_p t/\theta)$ curves for slow aggregation, $w_p < 1$, from the same curves for fast aggregation $w =$ constant $= 1$ (filled squares in Figure 3). This result shows that the Fuchs−Smoluchowski approximation of the constant aggregation probability $w = w_p$ overestimates the growth rate of the mean particle radius. This fact can be easily explained and reflects the noticeable decrease of the $w_{12}$ values (aggregation probability for particles with radius $r_1$ and $r_2$) in the course of the aggregation compared with the initial value $w_p$. The fastest kinetics of the mean radius growth was observed for unrestricted (fast) aggregation at $w = w_p = 1$. The data demonstrated that the enhancement of the electrostatic repulsion, related to the increase of the Debye length $\lambda$ or $\zeta$-potential, resulted in a retardation of the radius growth. Figure 4 shows examples of numerically calculated courses of the mean particle radius $r_m$ versus $\zeta$-potential and Hamaker constant $A$ for a long time of aggregation, $t/\theta = 10^9$. It follows from eq 8 that, at initial volume fraction $\varphi = 0.1$, $\theta \approx 7.6 \times 10^{-6}$ s and time $t = 7.6 \times 10^3$ s, which corresponds approximately to 2 h.

The mean particle radius $r_m$ was a decreasing function of both $\zeta$-potential and $\lambda$ values, which reflects an increase of repulsive forces between particles. It is interesting that the $r_m(\lambda)$ dependence was not very pronounced at large $\lambda$ (here $\geq 2$ nm). At a certain critical value of the Hamaker constant (here $A \geq 6 \times 10^{-20}$ J) the value of $r_m$ reached saturation, which corresponds to the $r_m$ value of fast aggregation ($w = w_p =$ constant $= 1$). Therefore, the large attraction forces can result in aggregation behavior similar to fast aggregation even at a long time (here $t/\theta < 10^9$). The distribution

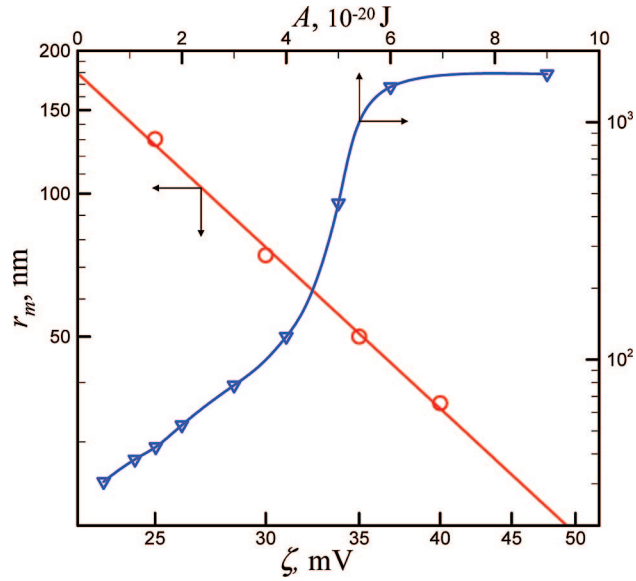


**Figure 4.** Mean radius of particle $r_m$ versus $\zeta$-potential ($\lambda = 2$ nm, $A = 10^{-20}$ J) and Hamaker constant $A$ ($\zeta = -40$ mV, $\lambda = 2$ nm) at long time of aggregation, $t/\theta = 10^9$.

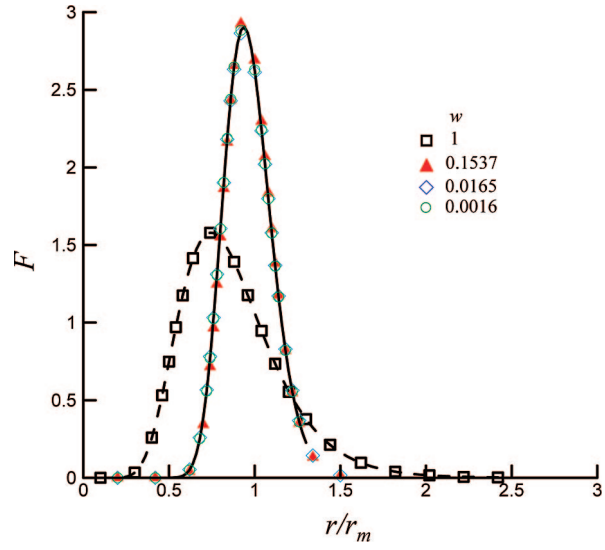


**Figure 5.** Particle radius distribution functions at $t/\theta = 10^6$ for the models of fast aggregation ($w =$ constant $= 1$, dashed line) and slow aggregation, $\zeta = -40$ mV, $A = 1 \times 10^{-20}$ J, $w_p = 0.1537$ ($\lambda = 1$ nm), $w_p = 0.0165$ ($\lambda = 2$ nm), and $w_p = 0.0016$ ($\lambda = 5$ nm).

functions $F$ of the relative particle radius $r/r_m$ at long times of aggregation $t/\theta \gg 1$ were significantly different for the fast and slow models of aggregation, which is shown in Figure 5. The fast model of aggregation (for sticking probability $w = 1$) produced wide distribution of the particle radii obeying the distribution function $F$, which noticeably deviated from the Gaussian shape and had a maximum at $r/r_m < 1$. It seems that the distribution function for the slow model of aggregation has a Gaussian-like shape with a maximum located near $r/r_m \approx 1$. The distribution functions demonstrate a rather universal shape, practically independent of $\lambda$ and $\zeta$-potential in the limit of very large values of $t/\theta$.

The time behavior of the relative width of the radius distributions $\Delta r/r_m$ was also rather different for the models of fast and slow aggregation. For fast aggregation the value of $\Delta r/r_m$ initially increased with time $t/\theta$ and then reached a plateau at $t/\theta \geq 10$, which is shown in Figure 6. At the same time, the relative width $\Delta r/r_m$ went through a maximum for

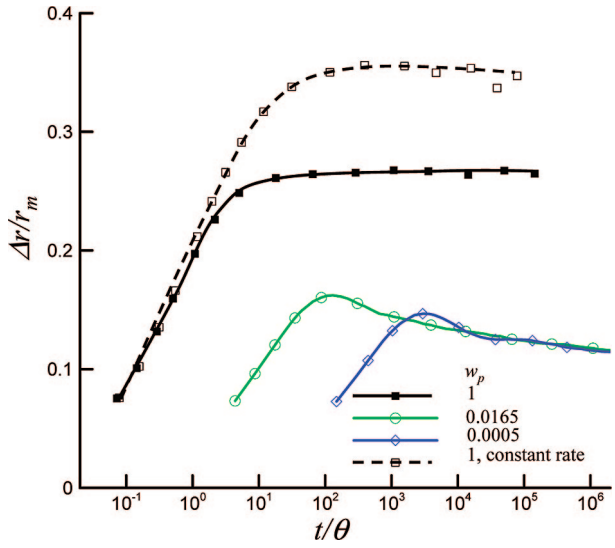


**Figure 6.** Time dependence of the relative width $\Delta r/r_m$ of the particle size distribution function $F$ for models of fast aggregation versus $t/\theta$, estimated at $A = 1 \times 10^{-20}$ J and $\zeta = -40$ mV, for different initial values of the aggregation probability $w = w_p = 1 =$ constant (model of fast aggregation), $w_p = 0.0165$ ($\lambda = 2$ nm), and $w_p = 0.0005$ ($\lambda = 9$ nm). Dashed line corresponds to the model of fast aggregation ($w = w_p = 1$) with constant rate; i.e., diffusion coefficient was set constant irrespectively of the size of particle.

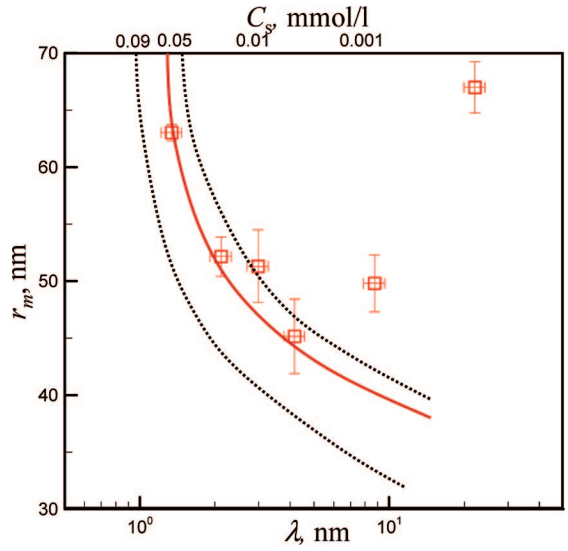


**Figure 7.** Mean particle radius $r_m$ (at $t/\theta = 10^9$) versus Debye length $\lambda$ (lower axis) or salt concentration $C_s$ (upper axis) of PDADMAC/PSS secondary PEC particles. The solid line corresponds to results of computer simulation for the following set of parameters: $A = 0.3 \times 10^{-20}$ J, $\zeta = -30$ mV. Lower dotted line: $A = 0.3 \times 10^{-20}$ J, $\zeta = -35$ mV. Upper dotted line: $A = 0.5 \times 10^{-20}$ J, $\zeta = -30$ mV.

the slow aggregation model. The position of the maximum $t/\theta$ depended on the values of initial aggregation probability $w_p$ (values $A$, $\lambda$, and $\zeta$-potential). It is interesting that different $\Delta r/r_m(t/\theta)$ dependences practically lay on the same descending curve at a long time of aggregation $t/\theta \gg 1$.

**Experimental Results.** ***Influence of Debye Length and Molecular Weight.*** Figure 7 presents experimental results on the influence of the Debye length $\lambda$ on the mean particle radius $r_m$. The total time of aggregation was approximately 2 h. The Debye length in the PEL solution $\lambda$ was estimated from the following equation:[25]

$$\lambda = [4\pi N_A l_B(\chi^{-1}C_{PEL} + 2C_s)]^{-1/2} \quad (9)$$

where $C_{PEL}$ is the PEL concentration, $C_s$ is the salt (NaCl) concentration, $l_B$ is the Bjerrum length ($l_B = 0.712$ nm in water), $N_A$ is the Avogadro constant, and $\chi$ is the Manning parameter.

As an approximation, we assumed $\chi = 2.69 \pm 0.26$ for PSS, which was calculated based on the relation $\chi = l_B/l_{eff}$, where $l_{eff}$ is the effective monomer length of PSS[26–30] as far as PSS is the excess PEL. The upper axis in Figure 7 presents the values of $C_s$ corresponding to the Debye length values $\lambda$ (lower axis), and horizontal error bars account for the uncertainties in estimation of the Manning parameter.

The mean particle radius $r_m$ goes through a minimum with Debye length in the PEL solution $\lambda$ increase (Figure 7). The particles were the smallest at certain $\lambda \approx \lambda_{min}$, and their size was larger for both $\lambda < \lambda_{min}$ and $\lambda > \lambda_{min}$. In this framework, the solid line in Figure 7presents one example of the simulated dependence with the adjusted values $\zeta = -30$ mV, $A = 0.3 \times 10^{-20}$ J, and aggregation time of, approximately, 2 h. The value of $\zeta = -30$ mV is in accordance with the experimental estimation for PEC particles at given conditions.[31] The adjusted value of $A$ for the PEC particles approximately corresponds to the expected value of the Hamaker constant for the polymer particles,[32] though more precise experimental data for the PEC particles are still unavailable.

The upper and lower dotted lines in Figure 7 correspond to the possible limits of mean particle radius $r_m$ variations with slightly different values of $\zeta$ and $A$. For $\lambda < \lambda_{min}$ the experimental points were found within the theoretically estimated limits, while the experimental points at $\lambda \approx 9$ nm and at $\lambda \approx 20$ nm are noticeably outside those limits. Hence, only the range of $\lambda < \lambda_{min}$ can be supported by our simulations on colloid aggregation. The nature of the observed $r_m$ increase with increase of $\lambda$ at $\lambda > \lambda_{min}$ is not fully resolved, so additional changes in the structure of both primary and secondary PEC particles must be considered. In that framework we assume an additional effect of $\lambda$ on the conformation of the involved PEL in terms of stretching for higher $\lambda$ and coiling for lower $\lambda$, which for the moment is beyond the scope of our present colloid simulation concept.

Conclusively, the general $\lambda$ dependence of the PEC particle size consists of two regimes: One related to the classical DLVO part treatable by our concept (denoted as the *colloid regime*) and one to the PEL conformation part (denoted as the *PEL regime*). Concerning the colloid regime, the increase of $r_m$ with decreasing $\lambda$ can be successfully described by simulation data at certain adjusted values of $A$ and $\zeta$ and mainly is due to enhancement of the dispersive interactions upon electrostatic screening increase.

***Shape of the Particle Size Distribution.*** Examples of the experimental particle size distribution functions $F$ are presented in Figure 8 for different salt concentrations. It should be noted that practically all the measured distribution functions $F$ displayed approximately the same universal form in the terms of $F$ versus $r/r_m$, but their widths (Figure 8) were surprisingly large compared to the widths of the simulated distribution functions (Figure 5). The relative width $\Delta r/r_m$ of the experimental particle size distribution function $F$ is $\Delta r/r_m \approx 0.9$, and the Smoluchovskii model of fast aggregation predicts $\Delta r/r_m \approx 0.27$. This may suggest a more complex aggregation behavior in real PEC systems in comparison to the results of the present computer simulation model, which is based only on three different parameters. A more complex model accounting for the presence of a disaggregation mechanism and distribution of $A$ and $\zeta$ parameters might be considered in the future.

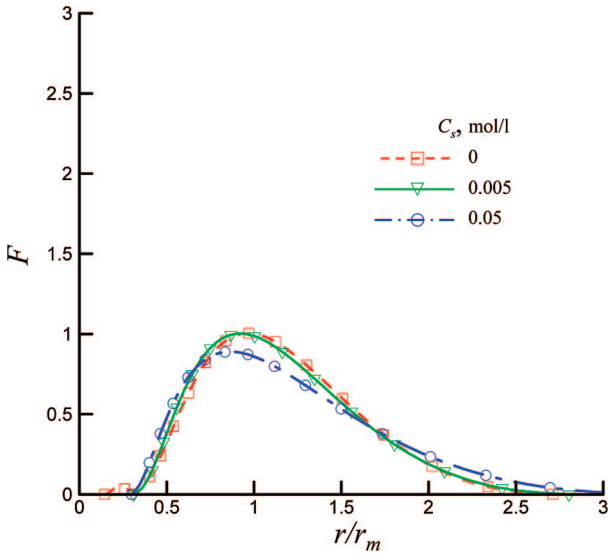


**Figure 8.** Particle radius distribution functions at different salt concentrations.

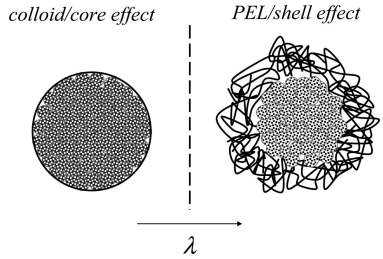


**Figure 9.** Schematic presentation of the effects of Debye length $\lambda$ on size and structure of aggregated PEC nanoparticles.

***Proposed Scheme of Aggregation.*** Based on our simulation and experimental results in the colloid regime and our assumption concerning the PEL regime, a scheme is proposed in Figure 9 showing qualitatively how the salt addition influences aggregation of the primary particles and the structure of the final secondary PEC particles. Our proposition is based on the accepted model of PEC particles consisting of a charged shell of excess PEL surrounding the charge-compensated core consisting of ion pairs between PA and PC as it is, e.g., claimed therein.[33] Generally, when these PEC particles are formed in the presence of salt, electrostatic interactions are screened on both regimes, PEL and colloid regime, respectively, as pointed out above.

The $\lambda$ increase in the interval of $\lambda \leq \lambda_{min}$ results in a weakening of colloid aggregation (colloid regime), and causes a decrease in the number of primary particles participating in final PEC aggregates (or decrease of $r_m$). For aggregation of particles in the interval of $\lambda > \lambda_{min}$, an increase of $\lambda$ causes a shell width increase (due to the salt dependence of the PEL molecule size[34,35]), resulting in an increase of $r_m$ (PEL regime).

## Conclusions

A new DLVO-based computer simulation model describing the aggregation of small charged primary particles to larger secondary colloid particles is developed. The proposed model allows overcoming of restrictions of the Fuchs−Smoluchowski approximation and accounts for changes of the Fuchs stability ratio during aggregation. It was shown that the Fuchs−Smoluchowski approximation results in an overestimation of the growth rate. The new simulation model of slow aggregation of the charged particles predicts that the relative width of the size distribution function $\Delta r/r_m$ goes through a maximum with increasing aggregation time, i.e., that the particle size distribution tends to become more homogeneous.

Experimental data for the formation of closely related PEC nanoparticles show that the radius of the PEC particles $r_m$ initially decreases with increasing Debye length $\lambda$, then goes through minimum (at certain $\lambda = \lambda_{min} \approx 3$–5 nm), and again starts to increase. The experimental findings on the increase of PEC particle size with decreasing Debye length in the regime $\lambda < \lambda_{min}$ was in good accordance with the computer simulation data based on the adjustable parameters $A$ and $\zeta$. In this so-called colloid regime ($\lambda > \lambda_{min}$), mainly aggregation of primary particles via short-range dispersive interactions occurs. The PEL regime ($\lambda > \lambda_{min}$) could not be described by our simulation concept, since $\lambda$ additionally influences the PEL conformation in terms of stretching for $\lambda > \lambda_{min}$ and coiling for $\lambda < \lambda_{min}$ resulting in larger or smaller particle sizes, respectively.

It is expected that PEC particles with the same final average size but formed either at high ($\lambda < \lambda_{min}$) or at low ($\lambda > \lambda_{min}$) ionic strength should have different structural densities. In principle, the more expanded structure of particles in the PEL regime can be tested by high-resolution transmission electron microscopic experiments, and we shall look into this in our future work.

**Acknowledgment.** Financial support from Deutsche Forschungsgemeinschaft (DFG, MU 1524/2-1) is gratefully acknowledged.

## References and Notes

(1) Ringsdorf, H. *Polym. Sci. Polym. Symp.* **1975**, *51*, 135.
(2) Antonietti, M.; Förster, S. *Adv. Mater.* **2003**, *15*, 1323.
(3) Donath, E.; Sukhorukov, G.; Caruso, F.; Davies, S.; Möhwald, H. *Angew. Chem., Int. Ed.* **1998**, *37*, 2201.
(4) Müller, M.; Kessler, B.; Richter, S. *Langmuir* **2005**, *21*, 7044.
(5) Müller, M.; Reihs, T.; Ouyang, W. *Langmuir* **2005**, *21*, 465.
(6) Family, F.; Popescu, M. N.; Amar, J. G. *Physica A* **2002**, *306*, 129.
(7) Family, F.; Meakin, P.; Vicsek, T. *J. Chem. Phys.* **1985**, *83*, 4144.
(8) Ziff, R. M.; McGrady, E. D.; Meakin, P. *J. Chem. Phys.* **1985**, *82*, 5269.
(9) Mulholland, G. W.; Mountain, R. D. *J. Chem. Phys.* **1986**, *84*, 4109.
(10) Ruckenstein, E.; Djikaev, Y. S. *Adv. Colloid Interface Sci.* **2005**, *118*, 51.
(11) Urbina-Villalba, G.; Lozsán, A.; Toro-Mendoza, J.; Rahn, K.; García-Sucre, M. *J. Mol. Struct.: Theochem* **2006**, *769*, 171.
(12) Fukasawa, T.; Adachi, Y. *J. Colloid Interface Sci.* **2006**, *304*, 115.
(13) Runkana, V.; Somasundaran, P.; Kapur, P. C. *Chem. Eng. Sci.* **2006**, *61*, 182.
(14) Zhang, N.; Zheng, Z. C. *J. Phys. D: Appl. Phys.* **2007**, *40*, 2603.
(15) Fuchs, N. A. *Z. Phys. Chem.* **1934**, *171*, 199.
(16) Russel, W. B.; Saville, D. A.; Schowalter, W. R. *Colloidal Dispersions*; Cambridge University Press: Cambridge, 1989.
(17) Higashitani, K.; Kondo, M.; Hatade, S. *J. Colloid Interface Sci.* **1991**, *142*, 204.
(18) Verwey, E. J. W.; Overbeek, J. Th. G. *Theory of the Stability of Lyophobic Colloids*; Elsevier: Amsterdam, 1948.
(19) Hogg, R.; Healy, T. W.; Fuerstenau, D. W. *Trans. Faraday Soc.* **1966**, *66*, 1638.
(20) Smoluchowski, M. *Z. Phys. Chem.* **1917**, *92*, 129.
(21) Atkins, P. W. *Physical Chemistry*; Oxford University Press: Oxford, 1995.
(22) Lebovka, N. I.; Ivanenko, Ya. V.; Vygornitskii, N. V. *Europhys. Lett.* **1998**, *41*, 19.
(23) Ivanenko, Y. V.; Lebovka, N. I.; Vygornitskii, N. V. *Eur. Phys. J. B* **1999**, *11*, 469.
(24) Kim, A. Y.; Hauch, K. D.; Berg, J. C.; Martin, J. E.; Anderson, R. A. *J. Colloid Interface Sci.* **2003**, *260*, 149.
(25) Wandrey, C.; Hunkeler, D.; Wendler, U.; Jaeger, W. *Macromolecules* **2000**, *33*, 7136.
(26) Carrière, D.; Dubois, M.; Schönhoff, M.; Zemb, T.; Möhwald, H. *Phys. Chem. Chem. Phys.* **2006**, *8*, 3141.
(27) Stukan, M.; Lobaskin, V.; Holm, C.; Vinogradova, O. *Phys. Rev. E* **2006**, *73*, 021801.

(28) Romet-Lemonne, G.; Daillant, J.; Guenoun, P.; Yang, J.; Holley, D. W.; Mays, J. W. *J. Chem. Phys.* **2005**, *122*, 064703.

(29) Grüner, F.; Lehmann, W. P.; Fahlbusch, H.; Weber, R. *J. Phys. A: Math. Gen.* **1981**, *14*, 307.

(30) McAloney, R.; Sinyor, M.; Dudnik, V.; Goh, C. *Langmuir* **2001**, *17*, 6655.

(31) Moya, S.; Ilie, A.; Bendall, J.; Hernandez-Lopez, J.; Ruiz-Garcia, J.; Huck, W. *Macromol. Chem. Phys.* **2007**, *208*, 603.

(32) Israelachvili, J. N. *Intermolecular and Surface Forces*, 2nd ed.; Academic Press: New York, 1997.

(33) Dautzenberg, H. *Macromolecules* **1997**, *30*, 7810.

(34) Peitzsch, R. M.; Burt, M. J.; Reed, W. F. *Macromolecules* **1992**, *25*, 806.

(35) Beer, M.; Schmidt, M.; Muthukumar, M. *Macromolecules* **1997**, *30*, 8375.

JP800581Y